Procedure for Separating Noise Sources in Measurements of Turbofan Engine Core Noise

Jeffrey Hilton Miles
Glenn Research Center, Cleveland, Ohio

NASA STI Program . . . in Profile

Since its founding, NASA has been dedicated to the advancement of aeronautics and space science. The NASA Scientific and Technical Information (STI) program plays a key part in helping NASA maintain this important role.

The NASA STI Program operates under the auspices of the Agency Chief Information Officer. It collects, organizes, provides for archiving, and disseminates NASA's STI. The NASA STI program provides access to the NASA Aeronautics and Space Database and its public interface, the NASA Technical Reports Server, thus providing one of the largest collections of aeronautical and space science STI in the world. Results are published in both non-NASA channels and by NASA in the NASA STI Report Series, which includes the following report types:

- TECHNICAL PUBLICATION. Reports of completed research or a major significant phase of research that present the results of NASA programs and include extensive data or theoretical analysis. Includes compilations of significant scientific and technical data and information deemed to be of continuing reference value. NASA counterpart of peer-reviewed formal professional papers but has less stringent limitations on manuscript length and extent of graphic presentations.

- TECHNICAL MEMORANDUM. Scientific and technical findings that are preliminary or of specialized interest, e.g., quick release reports, working papers, and bibliographies that contain minimal annotation. Does not contain extensive analysis.

- CONTRACTOR REPORT. Scientific and technical findings by NASA-sponsored contractors and grantees.

- CONFERENCE PUBLICATION. Collected papers from scientific and technical conferences, symposia, seminars, or other meetings sponsored or cosponsored by NASA.

- SPECIAL PUBLICATION. Scientific, technical, or historical information from NASA programs, projects, and missions, often concerned with subjects having substantial public interest.

- TECHNICAL TRANSLATION. English-language translations of foreign scientific and technical material pertinent to NASA's mission.

Specialized services also include creating custom thesauri, building customized databases, organizing and publishing research results.

For more information about the NASA STI program, see the following:

- Access the NASA STI program home page at *http://www.sti.nasa.gov*

- E-mail your question via the Internet to *help@sti.nasa.gov*

- Fax your question to the NASA STI Help Desk at 301–621–0134

- Telephone the NASA STI Help Desk at 301–621–0390

- Write to:
  NASA STI Help Desk
  NASA Center for AeroSpace Information
  7121 Standard Drive
  Hanover, MD 21076–1320

Procedure for Separating Noise Sources in Measurements of Turbofan Engine Core Noise

Jeffrey Hilton Miles
Glenn Research Center, Cleveland, Ohio

National Aeronautics and
Space Administration

Glenn Research Center
Cleveland, Ohio 44135

May 2006

Level of Review: This material has been technically reviewed by technical management.

Available from

NASA Center for Aerospace Information
7121 Standard Drive
Hanover, MD 21076–1320

National Technical Information Service
5285 Port Royal Road
Springfield, VA 22161

Available electronically at http://gltrs.grc.nasa.gov

Procedure for Separating Noise Sources in Measurements of Turbofan Engine Core Noise

Jeffrey Hilton Miles
National Aeronautics and Space Administration
Glenn Research Center
Cleveland, Ohio 44135

Abstract

The study of core noise from turbofan engines has become more important as noise from other sources like the fan and jet have been reduced. A multiple microphone and acoustic source modeling method to separate correlated and uncorrelated sources has been developed. The auto and cross spectrum in the frequency range below 1000 Hz is fitted with a noise propagation model based on a source couplet consisting of a single incoherent source with a single coherent source or a source triplet consisting of a single incoherent source with two coherent point sources. Examples are presented using data from a Pratt and Whitney PW4098 turbofan engine. The method works well.

Nomenclature

A	amplitude
B	amplitude of a point source B
B_e	resolution bandwidth,Hz.,$B_e = 1/T_d = r/NP = 11.71875 Hz$
c_o	speed of sound, m/sec
E	expected value
f	frequency
$F[]$	two sided Fourier transform operator
f_c	upper frequency limit,$f_c = 1/2\Delta t = r/2$, Hz. (24000 Hz.)
$G_{xx}(f)$	auto power spectral density function defined for non-negative frequencies only (one-sided)
$G_{xy}(f)$	cross power spectral density function defined for non-negative frequencies only (one-sided)
j	positive imaginary square root of -1,$\sqrt{-1}$
k	wavenumber
L_y	number of frequencies, $f_c/\Delta f = N/2$ (2048)
MW	molecular weight of air, 0.02897, $\frac{\text{kg}}{\text{mol}}$
N	amplitude of uncorrelated noise source
NP	segment length, number of data points per segment (4096)
n_d	number of disjoint (independent) segments,$n_d = B_e T_{total}$=234
n_o	number of overlapped segments/blocks
$p(t)$	pressure wave function
P_I	probability confidence interval, percent
$\Re$	gas constant, 8.314, $\frac{\text{Joule}}{\text{mole K}}$
r	radial distance, r
r	sample rate,samples/sec. (48000)
$R_{xx}(\tau)$	auto-correlation function
$R_{xy}(\tau)$	cross-correlation function
S_{xx}	two sided auto spectral density function
S_{xy}	two sided cross spectral density function
T_{total}	total record length,sec.($\approx$ 20 sec.)

t	time, sec.
T_d	record length of segment
TF	air temperature degrees Fahrenheit(80°)
TK	temperature in degrees Kelvin
$X(f)$	two sided Fourier transform
$X_\theta(i,f)$	one sided Fourier transform of block i

Subscripts

o	some arbitrary specific value
x	signal x
y	signal y

Symbols

Δf	frquency step, $1/T_d$,Hz. (11.718)
Δt	sampling interval,$1/r$ (1/48000),sec.
δ	dirac delta function
γ	ratio of specific heats, 1.4
$\gamma^2_{nn}(f)$	magnitude squared coherence (MSC) function of noise
$\gamma^2_{xy}(f)$	magnitude squared coherence (MSC) function
τ	time displacement, sec.
τ_1	propagation time delay

I.   Introduction

Understanding turbofan engine noise is a key priority of the National Aeronautics and Space Administration (NASA). Consequently, new diagnostic procedures to identify dominant sources and changes in dominant sources are being developed. This paper discusses a new diagnostic procedure that separates correlated far field turbofan noise from uncorrelated farfield turbofan noise using a multiple microphone method and point source acoustic models. The auto and cross spectrum in the frequency range below 1000 Hz is fitted with a noise propagation model based on a source couplet consisting of a single incoherent source with a single coherent source or a source triplet consisting of a single incoherent source with two coherent point sources. Two noise signals are coherent if they can be aligned with one another so that the coherence calculated using a periodogram averaging method is greater than the coherence of two random signals using the same periodogram averaging method. As fan noise and jet noise from turbofan engines are reduced, the issue of core noise reduction becomes more important. While core noise may be reduced by acoustic liners, the issue of measuring the amount of reduction becomes increasingly important. The proposed scheme separates coherent noise from random jet noise and should enable the measurement of the effectiveness of core noise reduction liners. The scheme was developed as part of a research program to study core noise from a Pratt & Whitney PW4098 turbofan engine (Miles.[1–3])

Procedures using coherence-based techniques have been developed for extracting acoustic signals buried in noise. The coherent output power method for noise source identification is discussed in by Bendat.[4–6]The application of this technique that is of interest is the use of coherent output power spectra to separate and identify correlated combustion noise in far field measurements of turbofan engine noise. Karchmer[7] and Karchmer, Reshotko, and Montegani,[8] use the coherence function calculated from internal microphone measurements of fluctuating pressures in the combustor and far field acoustic pressures to determine the correlated combustion noise of a YF102 turbofan engine at far field locations by calculating the coherent output power spectrum.

The three signal coherence technique was developed by Chung[9, 10] for flow noise rejection. A similar technique was developed and used by Krejsa.[11] The three signal coherence technique was used by Shivashankara[12] to study core noise in a Pratt and Whitney JT9D. It was used by Hsu and Ahuja[13] to separate ejector internal mixing noise from far field measurements and by Stoker, Ahuja, and Hsu[14] to separate wind-tunnel background noise and wind noise from automobile interior noise measurements. It was used by Michalke, Arnold and Holste[15]to study sound in a circular duct with mean flow. The method is also discussed by Minami and Ahuja.[16]

The inherent coherent properties of jet and core noise have been used in several source separation procedures. The radiated field of jet noise is has a low coherence when measured at two widely separated points.

Parthasarathy[17] attributes this to the fact that the jet noise sources are in motion so that the source frequencies undergo large Doppler shifts as the noise is radiated to the far field. Core noise has a high coherence when measured at two widely separated points. This is attributed to the fact that the frequencies of the radiated core noise are preserved unchanged in the far field Parthasarathy.[17] Consequently, three signal coherence technique is especially useful to study turbofan core noise using widely spaced microphones.

A method of separating jet noise and core noise using auto-correlations and cross-correlations was developed by Parthasarathy.[17] The model presented assumes the microphones are located on the arc of a circle about a single source having a known position. This is a couplet source which produces a core noise sound radiation field that is correlated over wide microphone spacing and a jet noise sound radiation field that is not correlated over wide microphone spacing. Since the microphones are on the same arc, the model cross-correlations calculated have zero propagation time delay. In addition, a model for the jet noise directivity is used. The resulting system of three unknowns and three equations can be solved exactly. In applying this method to data from a small jet the source location is known and a correction to the amplitude correlation measurements is made so that the microphones are located on the arc of a circle about a source having a known position. In applying this method to measured data, I assume the cross-correlations were also time shifted to remove the propagation time delay. An extension of the method to obtain spectral information is also discussed using non zero values of propagation time delay. The phase angle shift due to propagation time delay is not discussed. Again, this seems to indicate that the propagation time delay is being set to zero. The method calculates the jet noise spectrum, the core noise spectrum, and the directivity ratio of the core noise at a particular angle as a function of frequency from measured auto and cross spectra. The method was applied to experimental data obtained in a small scale facility. The spectral formulation of this method was used by Tessson[18, 19] to study jet noise and core noise from the static test of a small gas turbine engine in an anechoic chamber.

A method to achieve separation of two different correlated noise sources from far field measurements contaminated by extraneous jet noise using multiple microphones was developed by Minami and Ahuja.[16] The equations discussed use measured auto-spectra and cross-spectra. The model assumes the source noise can be represented by a triplet consisting of a correlated noise source A, correlated noise source B, and an uncorrelated noise source. I assume that all the sources are at a single triplet location however in the formulation presented no source location or microphone location information is used. The five microphone method described involves solving a set of 55 equations for 55 unknowns at each frequency of interest. At each microphone location the spectrum of correlated noise source A, correlated noise source B, and an uncorrelated noise source is obtained as a function of frequency. The method was validated using analytical simulations.

The method presented herein also models the auto- and cross- spectrum measurements made with multiple microphones. The method uses a point source propagation model so the microphones need not be on an arc. As a consequence, the directivity is the same in each direction for each source. The method assumes the engine noise source can be modeled with a source doublet or triplet. One part source doublet and triplet consists of an incoherent source at the location taken as $x = 0.0$ and $y = 0.0$. The source doublet has an additional coherent source at location $x = x_A$ with $y = 0.0$. The source triplet has two additional coherent sources at location $x = x_A$ with $y = 0.0$ and $x = x_B$ with $y = 0.0$. As part of the procedure a comparison of results obtained with the use of a source couplet with the results obtained using a source triplet is made. In addition, a source position is assumed to have a y coordinate of zero and the x coordinate along the engine axis is found as a function of frequency. This is done since noise can be radiated from the engine case to the far field as well as from the nozzle. In order to solve the resulting acoustic equations for a small set of parameters, a solution method that provides an optimum solution in a least square sense without derivatives was used. The method is set up to do a least squares curve fit to match the auto-spectra and the cross spectra magnitude and phase measurements between all microphones. The method assumes the existence of one or more point sources that can produce the same measurements. The problem then becomes one of finding the appropriate point sources. The current strategy is to have the curve fit adjust the amplitude and x location of the sources that determine the cross spectrum at each microphone and the amplitude of a random noise source. For the single coherent source case, three parameters are found at each frequency. When a model with two coherent sources is used, one has five parameters to determine at each frequency. Examples are presented calculated with a four microphone array using data from a Pratt and Whitney PW4098 turbofan engine.

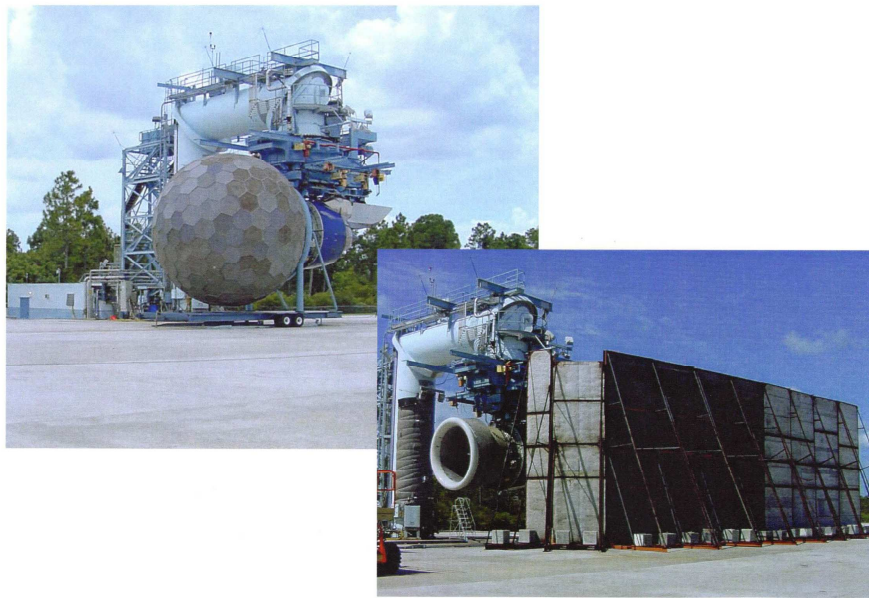**PW4098 Engine at C-11 Stand for EVNRC Phase 2 Tests**

Figure 1.   Pratt & Whitney test stand C11, West Palm Beach Florida, with PW4098 engine and attached acoustic inflow control device also with and without aft acoustic barrier walls for EVNRC Phase 2 tests.

II. Analysis Method

The core noise is assumed to be propagating in acoustic modes in the turbofan engine. The coherent acoustic energy leaves the nozzle and travels through the turbofan engine shear layer to a ground microphone. Additional acoustic energy from the jet and from random scattering reaches the same microphone. In this test program four microphones at 150 feet and angular position of $100^o, 110^o, 120^o$ and 130° measured from the inlet were used. Consequently, the measurements available at each test condition are four sound pressure spectrums and six sound pressure cross-spectrums each consisting of a magnitude and a phase angle. These sixteen measurements are available as a function of frequency. Four real variable and six complex variable acoustic equations relate the measurements and the model parameters. The angular separation of at least 10 degrees means that the jet noise measured at any microphone can be assumed to be incoherent with the jet noise at any another microphone.

The basic procedure is to assume that some combination of coherent sources and an incoherent source will produce the measured auto and cross spectra. The coherent source is assumed to be on the turbofan engine centerline as some x position to be determined with $y = 0$. The incoherent source is assumed to be at $x = 0$ and $y = 0$. Using the results in appendix A on page 11 where the one-sided spectrum functions for acoustic signals from a point source are derived, the acoustic model equations shown in appendix B through E are defined. The following models were considered.

Figure 2. Acoustic arena and microphone array at Pratt & Whitney test stand C11, West Palm Beach Florida for EVNRC Phase 2 tests.

- Two parameter model. Coherent source of magnitude A at $(x = x_a, y = 0)$ (Appendix B on page 12).

- Three parameter model. Coherent source of magnitude A at $(x = x_a, y = 0)$ (Appendix C on page 13). with an incoherent source of magnitude N at $(x = 0, y = 0)$

- Four parameter model. Coherent source of magnitude A at $(x = x_a, y = 0)$ and a Coherent source of magnitude B at $(x = x_b, y = 0)$ (Appendix D on page 13).

- Five parameter model. Coherent source of magnitude A at $(x = x_a, y = 0)$ and Coherent source of magnitude B at $(x = x_b, y = 0)$ with an incoherent source of magnitude N at $(x = 0, y = 0)$ (Appendix E on page 13)

Consequently, the number of equations greatly exceeds the number of model parameters used in the study discussed herein. Note that no radiation pattern is assumed for these models. These are point sources that radiate sound equally in all directions.

The measured auto-spectrum and cross-spectrum required as input to the acoustic model equations is experimentally determined and subject of nominal experimental error and statistical uncertainties. Also, the measured auto-spectrum includes random noise in addition to coherent signals from propagating waves. Consequently, a solution method that provides an optimum solution in a least squares sense without derivatives was used. Algorithms for minimization without derivatives are discussed by Brent.[20] The search technique used in this study is described by Powell[21] and Fortran computer code for this algorithm is given by Shapiro[22] and Kuester.[23] The code used was a modified version of the one in Shapiro[22] which was updated to be in a FORTRAN 90 style. The cost function used is written in terms of sound pressure level and phase angle.
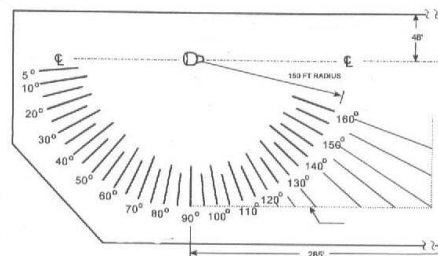
III.   Experiment

To demonstrate the usefulness of the procedure for separating correlated and uncorrelated noise sources measurements made in the far field of a Pratt & Whitney PW4098 turbofan engine will be used. The measurements were made in a study of aircraft turbofan engine core noise conducted as part of the NASA Engine Validation of Noise Reduction Concepts (EVNRC) Program.

The spectral estimate parameters are shown in table 1 on the next page The signal processing algorithms used were written in Fortran. They are based on subprogram modules developed by Stearns and David.[24] In the calculations the segments were overlapped by 50 percent. Fig. 1 on page 4 shows the test stand. Fig. 2 on the page before shows the angular placement of the far field microphones on a 150 foot radius. This analysis uses the microphones at 100°, 110°, 120° and 130° measured from the inlet. The coordinate system used herein has the x axis along the engine centerline increasing to the right. The y axis is perpendicular and increases toward the top of the page. The center $(x = 0, y = 0)$ is at the engine center.

IV.   Results

A.   Cross-Spectra Validity

The signals from each pair of microphones used to calculate the cross-spectra only produce valid measurements if the coherence is greater than some threshold coherence. The coherence function is given by

$$\gamma^2_{\theta_1\theta_2}(f) = \frac{|G_{\theta_1\theta_2}(f)|^2}{G_{\theta_1\theta_1}(f)G_{\theta_2\theta_2}(f)} \tag{1}$$

The measured coherence calculated using segments overlapped by 50 % is given by

$$\hat{\gamma}^2_{\theta_1\theta_2}(f) = \frac{|\sum_{i=1}^{n_o} X^*_{\theta_1}(i,f)X_{\theta_2}(i,f)|^2}{\sum_{i=1}^{n_o} |X_{\theta_1}(i,f)|^2 \sum_{i=1}^{n_o} |X_{\theta_2}(i,f)|^2} \tag{2}$$

In Miles[1] comparisons were made of a coherence threshold based on aligned and unaligned coherence and one based an analytical coherence threshold using computer simulation. Results were obtained from computer simulation that show good agreement with the theoretical estimate of the analytical coherence threshold

$$\gamma^2_{nn} = 1 - (1-P)^{1/(n_d-1)} \tag{3}$$

where we use herein $P = 0.95$ and instead of the number of independent segments/blocks n_d we take $n_d = n_o$ where n_o is the number of overlapped segments/blocks. The coherence threshold γ^2_{nn} is discussed by Carter,[25,26] Halliday et. al.[27] (page 247), and Brillinger[28] (page 317). The coherence threshold γ^2_{nn} has a value which is greater than 95 % of the values of the coherence of two independent time series calculated using n_d disjoint data segments/blocks. The coherence threshold used herein is calculated using the number of overlapped segments, n_o. As part of the set of figures for each case used to show the results, the coherence and the threshold coherence, γ^2_{nn}, will also be shown. The data used herein had coherence values above the threshold coherence, γ^2_{nn}.

B.   Cross-Spectra Phase Angle Sampling Errors

In Bendat[6] and in Piersol[29] the random error in the phase estimates due to statistical sampling is given in terms of the standard deviation of the estimated phase angle, $\hat{\theta}_{12}$, by

$$\sigma\left[\hat{\theta}_{12}(f)\right] \approx \sin^{-1}\left\{\frac{\left[1 - \gamma^2_{12}(f)\right]^{1/2}}{|\gamma_{12}|\sqrt{2n_o}}\right\} \tag{4}$$

where $\sigma\left[\hat{\theta}_{12}(f)\right]$ is measured in radians and as used herein n_o is selected to be the number of overlapped segments or blocks used in the spectral calculations. For the special case where the term in curly brackets is small Eq. 4 becomes

$$\sigma\left[\hat{\theta}_{12}(f)\right] \approx \frac{\left[1 - \gamma_{12}^2(f)\right]^{1/2}}{|\gamma_{12}|\sqrt{2n_o}} \tag{5}$$

where for the unknown coherence $\gamma_{12}^2(f)$ the estimated coherence $\hat{\gamma}_{\theta_1 \theta_2}^2(f)$ from Eq. 2 is used. A plot of the standard deviation of the phase angle in degrees verses coherence is shown in 3 on page 10.

When the coherence is greater than 0.15, Fig. 3 shows the standard deviation should be less than 5 degrees. Straight line fits was made to the phase verses frequency data. The standard deviation of the error was greater than on would calculate from the coherence i.e around 10 degrees when one calculated 5 degrees. Consequently, the phase angle measurements might be showing propagation effects due to wind shear or temperature gradients or a change in source location with frequency. In addition, the error verses frequency plots seemed to be in phase for each pair. As a consequence, instead of a using a fixed source location in the model the y co-ordinate of a source is fixed at zero and the x co-ordinate is free to vary.

C.   Point source models

The method discussed has been tried out over a range of operating conditions. For each case all four models were used. Four typical cases presented herein shown in Fig. 4 on page 14, Fig. 5 on page 15, Fig. 6 on page 16, and Fig. 7 on page 17.are for N1 Corr. values of 582 rpm, 1622 rpm, 1900 rpm and 2743 rpm. Only one acoustic model result is shown for each case. The selected case uses the fewest number of parameters to achieve a good result. For each case all four auto-spectra and six cross-spectra are calculated. However, only the following items are shown herein:

- The measured and calculated auto-spectrum at 100 degrees.

- The measured and calculated cross-spectrum magnitude between the 100 degree and 120 degree microphones.

- The measured and calculated cross-spectrum phase angle between the 100 degree and 120 degree microphones.

- The measured coherence and analytic threshold coherence between the 100 degree and 120 degree microphones.

- The sound pressure amplitude curve fit parameter or parameters.

- The correlated source location or locations.

In the modeling scheme used herein, for each case the jet noise is assumed to be uncorrelated between the microphones at all frequencies. Furthermore, it is assumed the basic radiation pattern of the correlated noise as specified by the cross-spectrum phase angle could be represented by a single point coherent source at some x location. In all cases, a better result is obtained by using an acoustic model which assumes a non correlated noise source is present and letting the computer solution procedure determine if its value is significant. In some cases a second coherent point source gives a slightly better result. Only the coherent sources create the cross spectra. The auto spectra are due to the coherent and incoherent sources.

The general formulation is given in Appendix A on page 11. The general models are shown in Appendix B on page 12 through E on page 13.

Table 1. Spectral Estimate Parameters

Parameter	value
Segment length i.e. Data points per segment, NP	4096
Sample rate, r, samples/second	48,000
Segment length, $T_d = NP/r$, seconds	0.08533
Sampling interval, $\Delta t = 1/r$, seconds	2.0833×10^{-5}
Frequency step, $\Delta f = 1/T_d$, Hz	11.718
Upper frequency limit, $f_c = 1/2\Delta t = r/2$,Hz	24000
number of frequencies, $Ly = f_c/\Delta f = NP/2$	2048
Time delay, $\tau = 6323/48000$,seconds	0.1317
number of independent samples	234
overlap	0.50
Sample length,sec.	20

1. *N1 Corr = 582 rpm*

At the N1 Corr 582 rpm operating condition the core noise is dominated by a low frequency combustion tone at 327 Hz as shown in Fig. 4a. The core noise radiation pattern is well represented by a single point source as shown in Fig. 4b and Fig. 4c. The results shown are for the three parameter couplet source model (A,N,x_a) described in Appendix C on page 13. As shown in Fig. 4a, at a few low frequency points the computer solution included a uncorrelated noise source. The coherence shown in Fig. 4d is above the coherence threshold $\gamma^2_{nn} = 0.00639431$. Consequently, the cross spectrum phase angles look good. At most points the uncorrelated noise level was to low to plot as shown in Fig. 4e. As shown in Fig. 4f, in order to match the measured phase angle the computer model puts the source at more than $x_a = 50$. feet for frequencies less than 200 Hz. and near $x_b = 20$ feet for frequencies greater than 200 Hz.

2. *N1 Corr = 1622 rpm*

At the N1 Corr 1622 rpm operating condition, results are shown for the five parameter triplet source model (A,B,N,x_a,x_b) described in Appendix E on page 13. As shown in Fig. 5a this model does a good job below 300 Hz. in representing the 100 degree microphone auto-spectrum and a satisfactory job at higher frequencies. At higher angles the curve fit at these frequencies is better. The core noise radiation pattern is well represented by a two point sources as shown in Fig. 5b and Fig. 5c. Below 300 Hz. this model does a fine job. The coherence shown in Fig. 5d is above the coherence threshold $\gamma^2_{nn} = 0.00639431$ below 800Hz. Below 400 Hz. the coherence is grater than 0.15. Consequently, the cross spectrum phase angles look good below 400 Hz. The variation of the two-point model correlated source amplitude shown in Fig. 5e and the source separation results shown in Fig. 5a have the same frequency dependence that the combustion modes have in that they seem to be in 200 Hz bands. This suggests the correlated noise is due to the combustor source. As shown in Fig. 5f, the source locations of the two point sources have an interesting symmetry. Source B is near $x_B = 0.0$ and may represent sound radiation from the engine case. Source A is near $x_A = 25$ and may represent sound radiation from the nozzle.

3. *N1 Corr = 1900 rpm*

Again, at the N1 Corr 1900 rpm operating condition, results are shown for the five parameter triplet source model (A,B,N,x_a,x_b) described in Appendix E on page 13. As shown in Fig. 6a this model does a good job below 200 Hz. in representing the 100 degree microphone auto-spectrum and a satisfactory job at higher frequencies. At higher angles the curve fit at these frequencies is better. The core noise radiation pattern is well represented by a two point sources as shown in Fig. 6b and Fig. 6c. The coherence shown in Fig. 6d is above the coherence threshold $\gamma^2_{nn} = 0.00639431$ below 800Hz. At most points below 800 Hz the coherence is grater than 0.10. Consequently, the cross spectrum phase angles look good below 800 Hz. The variation of the two-point model correlated source amplitude shown in Fig. 6e and the source separation results shown in Fig. 6a again have the same frequency dependence that the combustion modes have in that they seem to be in 200 Hz bands. This again suggests the correlated noise is due to the combustor source. Again. as shown in Fig. 6f, the source locations of the two point sources have and interesting symmetry. Source B is again near $x_B = 0.0$ and may represent sound radiation from the engine case. Source A is again near $x_A = 25$ and may represent sound radiation from the nozzle.

4. *N1 Corr = 2743 rpm*

The highest power setting examined herein is the N1 Corr. 2743 rpm operating condition. The auto-spectrum at 100 degrees is shown in Fig. 7a. Below 100 Hz. the uncorrelated noise source is not needed to represent the measurements. The core noise radiation pattern is well represented again by a single point source as shown in Fig. 7b and Fig. 7c. The results shown are for the three parameter couplet source model(A,N,x_a) described in Appendix C on page 13. As shown in Fig. 7a, at frequencies above 100 Hz. the computer solution included a uncorrelated noise source. The coherence shown in Fig. 7d is above the coherence threshold $\gamma^2_{nn} = 0.00639431$ below 200Hz. Below 200 Hz. the coherence is above 0.15. Consequently, the cross spectrum phase angles look good below 200 Hz. Below 100 Hz., the uncorrelated noise level was to low to plot as shown in Fig. 7e. As shown in Fig. 7f, in order to match the measured phase angle the computer model puts the source at more than $x_A = 30$ feet for frequencies less than 100 Hz. and less than $x_A = 30$ feet for frequencies greater than 100 Hz.

V. Discussion

These results show how important it is to start with no preconceived idea of what acoustic source mode best represents the measured turbojet core noise. One should use a model that best fits the data and not ones idea of the model. The results show the uncorrelated noise source is not important at frequencies less than 800 Hz at these angles. Furthermore, the results show that core noise dominates at frequencies less than 800 Hz at these angles. Furthermore, at many operating points, the sound radiation field can be attributed to two coherent core noise sources. The results indicate that one might be the engine case while the other is the nozzle. The variation of the two-point model correlated source amplitude shown in Fig. 4d and the source separation results shown in Fig. 4a have the same frequency dependence that the combustion modes have in that they seem to be in 200 Hz bands. This suggests the correlated noise is due to the combustor source. The variation of the two-point model correlated source amplitude shown in Fig. 5d and the source separation results shown in Fig. 5a have the same frequency dependence that the combustion modes have in that they seem to be in 200 Hz bands. This again suggests the correlated noise is due to the combustor source. Note however, that the cross-spectrum phase angle measurements shown in Figs 4c and 5c have a lot of dispersion. The need to satisfy this dispersion may be causing the two correlated source with uncorrelated noise five parameter model to perform better than single correlated source with noise three parameter model. Consequently, further studies need to be done to resolve this issue.

VI. Conclusions

A new method to separate correlated signals buried in turbofan engine core noise has been presented. The method is based on finding acoustic model coefficients that enable a system of equations based on one or two correlated noise sources and an uncorrelated noise source to reproduce experimental data. The effectiveness and the reliability of the method have been tested using Pratt and Whitney PW4098 far field acoustic measurements. The agreement achieved between the experimental data and the acoustic model used confirm the effectiveness of the procedure.
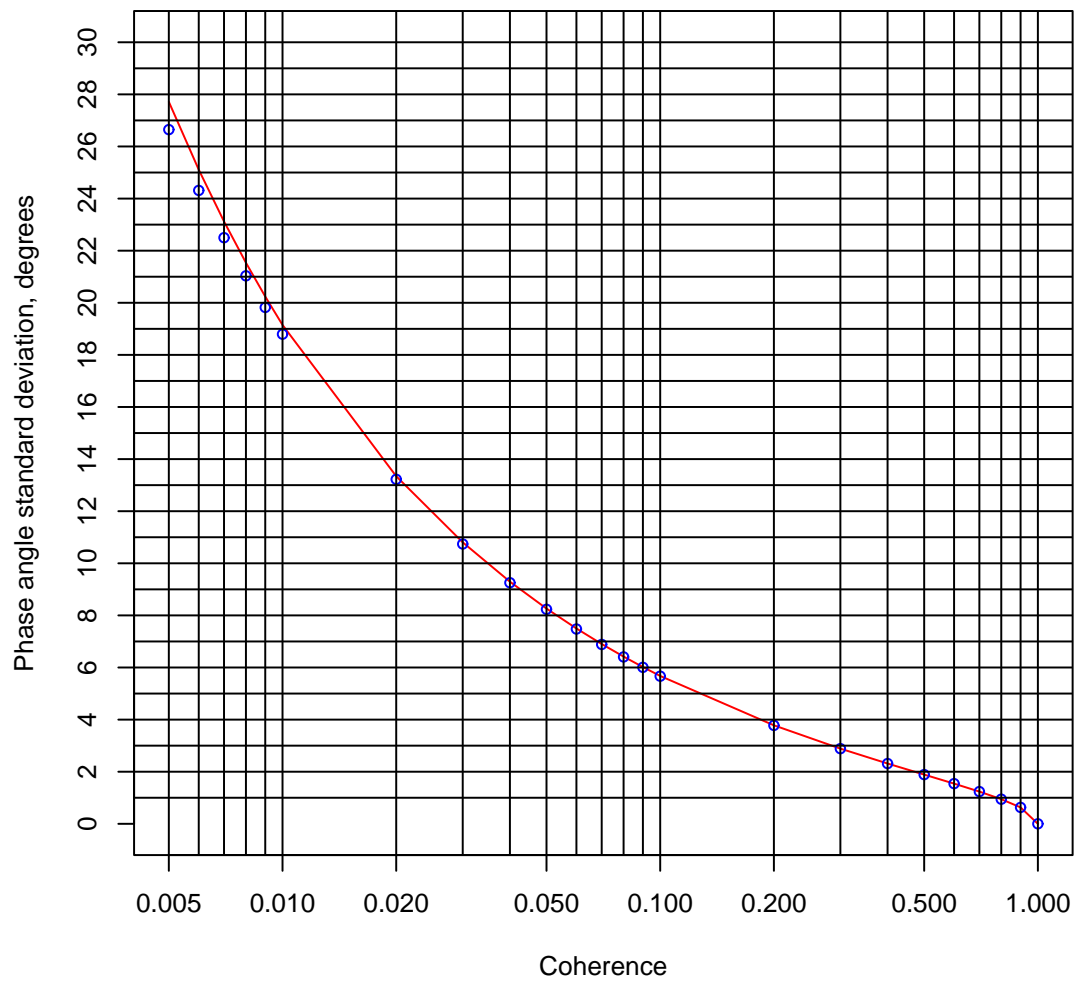
Figure 3. Standard deviation of phase angle of G_{34} based on γ_{34}^2 and n_o.

A. One-sided spectrum functions for acoustic signals from a point source

We shall assume a compact source region and assume the source produces a wave which spreads spherically outward with no preferred direction. The wave equation in this case as discussed by Morse[30] page 309 is

$$\frac{1}{r^2}\frac{\partial}{\partial r}\left(r^2\frac{\partial p}{\partial r}\right) = \frac{1}{c_o^2}\frac{\partial^2 p}{\partial t^2} \tag{6}$$

We shall assume a simple source solution to the wave equation $p(t) = \frac{A}{R}\exp(-ikR)\sin(2\pi f_0 t)$ where

$$
\begin{aligned}
k &= \frac{2\pi f_0}{c_o} \\
c_o^2 &= \frac{\gamma \Re T K}{MW}, \frac{m}{sec} \\
\Re &= 8.314, \frac{Joule}{mole\ K} \\
MW &= 0.02897\frac{kg}{mol} \\
TF &= 80
\end{aligned}
\tag{7}
$$

$$\tag{8}$$

To get the auto-spectrum and cross-spectrum of a point source we use the following relationships from correlation and spectral analysis texts by Bendat.[4–6]
The autocorrelation function of x is

$$R_{xx}(\tau) = E[x_k(t)x_k(t+\tau)] \tag{9}$$

The auto correlation function for a sum of two processes $y(t) = x_1(t) + x_2(t)$ is

$$
\begin{aligned}
R_{yy}(\tau) &= E[(x_1(t) + x_2(t))(x_1(t+\tau) + x_2(t+\tau))] \\
&= R_{x_1 x_1}(\tau) + R_{x_1 x_2}(\tau) + R_{x_2 x_1}(\tau) + R_{x_2 x_2}(\tau)
\end{aligned}
\tag{10}
$$

The two-sided auto and cross spectral density functions are

$$
\begin{aligned}
S_{xx}(f) &= F[R_{xx}(\tau)] = \int_{-\infty}^{\infty} R_{xx}(\tau)\exp(-j2\pi ft)dt \\
S_{xy}(f) &= F[R_{xy}(\tau)] = \int_{-\infty}^{\infty} R_{xy}(\tau)\exp(-j2\pi ft)dt
\end{aligned}
\tag{11}
$$

and of course we have the inverse relationships

$$
\begin{aligned}
R_{xx}(\tau) &= F^{-1}[S_{xx}(f)] = \int_{-\infty}^{\infty} S_{xx}(f)\exp(+j2\pi f\tau)df \\
R_{xy}(\tau) &= F^{-1}[S_{xy}(f)] = \int_{-\infty}^{\infty} S_{xy}(f)\exp(+j2\pi f\tau)df
\end{aligned}
\tag{12}
$$

The two-sided auto spectrum function for a sum of two processes $y(t) = x_1(t) + x_2(t)$ is

$$
\begin{aligned}
S_{yy}(f) &= F[E[(x_1(t) + x_2(t))(x_1(t+\tau) + x_2(t+\tau))]] \\
&= F[R_{x_1 x_1}(\tau) + R_{x_1 x_2}(\tau) + R_{x_2 x_1}(\tau) + R_{x_2 x_2}(\tau)] \\
&= S_{x_1 x_1}(\tau) + S_{x_1 x_2}(\tau) + S_{x_2 x_1}(\tau) + S_{x_2 x_2}(\tau)]
\end{aligned}
\tag{13}
$$

The auto-correlation function is the Fourier transform of the correlation of $x(t)$ with itself is related to the Fourier transform of $x(t)$ by

$$S_{xx}(f) \quad = \quad F[R_{xx}(\tau)] = \int_{-\infty}^{\infty} R_{xx}(\tau) \exp(-j2\pi f\tau) d\tau$$

$$= \quad X(f)X^*(f) \tag{14}$$

The cross-correlation function is the Fourier transform of the correlation of $x(t)$ and y(t) is related to the Fourier transform of $x(t)$ and $y(t)$ by

$$S_{xy}(f) \quad = \quad F[R_{xy}(\tau)] = \int_{-\infty}^{\infty} R_{xy}(\tau) \exp(-j2\pi f\tau) d\tau$$

$$= \quad X(f)Y^*(f) \tag{15}$$

The one-sided spectral density function is $G_x(f) = 2S_x(f) \ 0 \le f < \infty$.

The auto-correlation function of a sine wave $x(t) = A\cos(2\pi f_0 t)$ is

$$R_{xx} = \frac{A^2}{2}\cos(2\pi f_0) \tag{16}$$

The power spectral density of a sine wave $x(t) = A\cos(2\pi f_0 t)$ is

$$G_{xx} = \frac{A^2}{2}\delta(f - f_0) \tag{17}$$

The one-sided spectrum function for a sum of two processes $y(t) = x_1(t) + x_2(t)$ is

$$G_{yy}(f) \quad = \quad G_{x_1 x_1}(\tau) + G_{x_1 x_2}(\tau) + G_{x_2 x_1}(\tau) + G_{x_2 x_2}(\tau)] \tag{18}$$

Next, these relationships are applied to signals produced by acoustic waves from a point source and received at microphone i and j.

$$p_{a_i}(t) \quad = \quad \frac{A}{R_{a_i}} exp(ikR_{a_i}) \sin(2\pi f_0 t)$$

$$p_{a_j}(t) \quad = \quad \frac{A}{R_{a_j}} exp(ikR_{a_j}) \sin(2\pi f_0 t) \tag{19}$$

We have for the one-sided auto spectral density and the one-sided cross spectral density,

$$G_{p_{a_i} p_{a_i}} \quad = \quad \frac{1}{2}\frac{A^2}{R_{a_i}^2}\delta(f - f_0) \tag{20}$$

$$G_{p_{a_i} p_{a_j}} \quad = \quad \frac{1}{2}\frac{A^2}{R_{a_i} R_{a_j}}e^{-jk(R_{a_i} - R_{a_j})}\delta(f - f_0) \tag{21}$$

B.   Correlated noise source A

Consider the i'th and j'th microphones and a single point acoustic source.
As shown in Appendix A, the auto spectra are

$$G_{p_{a_i} p_{a_i}} \quad = \quad \frac{1}{2}\frac{A^2}{R_{a_i}^2}\delta(f - f_0) \tag{22}$$

$$G_{p_{a_j} p_{a_j}} \quad = \quad \frac{1}{2}\frac{A^2}{R_{a_j}^2}\delta(f - f_0) \tag{23}$$

and the cross spectrum is

$$G_{p_{a_i} p_{a_j}} \quad = \quad \frac{1}{2}\frac{A^2}{R_{a_i} R_{a_j}}e^{-jk(R_{a_i} - R_{a_j})}\delta(f - f_0) \tag{24}$$

## C.   Correlated noise source A and uncorrelated source N

Consider the i'th and j'th microphones, a single point acoustic source A and a noise source N.
As shown in Appendix A, the auto spectra are

$$G_{p_{a_i} p_{a_i}} = \frac{1}{2} \frac{A^2}{R_{a_i}^2} \delta(f - f_0) + \frac{1}{2} \frac{N^2}{R_{n_i}^2} \delta(f - f_0) \tag{25}$$

$$G_{p_{a_j} p_{a_j}} = \frac{1}{2} \frac{A^2}{R_{a_j}^2} \delta(f - f_0) + \frac{1}{2} \frac{N^2}{R_{n_j}^2} \delta(f - f_0) \tag{26}$$

and the cross spectrum is

$$G_{p_{a_i} p_{a_j}} = \frac{1}{2} \frac{A^2}{R_{a_i} R_{a_j}} e^{-jk(R_{a_i} - R_{a_j})} \delta(f - f_0) \tag{27}$$

D.   Correlated noise source A and correlated noise source B

Consider the i'th and j'th microphones, a point acoustic source A and a point acoustic source B.
As shown in Appendix A, the auto spectra are

$$G_{p_{a_i} p_{a_i}} = \frac{1}{2} \frac{A^2}{R_{a_i}^2} \delta(f - f_0) + \frac{1}{2} \frac{B^2}{R_{b_i}^2} \delta(f - f_0) \tag{28}$$

$$G_{p_{a_j} p_{a_j}} = \frac{1}{2} \frac{A^2}{R_{a_j}^2} \delta(f - f_0) + \frac{1}{2} \frac{B^2}{R_{b_j}^2} \delta(f - f_0) \tag{29}$$

and the cross spectrum is

$$G_{p_i p_j} = \frac{1}{2} \frac{A^2}{R_{a_i} R_{a_j}} e^{-jk(R_{a_i} - R_{a_j})} \delta(f - f_0) + \frac{1}{2} \frac{B^2}{R_{b_i} R_{b_j}} e^{-jk(R_{b_i} - R_{b_j})} \delta(f - f_0) \tag{30}$$

E.   Correlated noise source A, correlated noise source B, and uncorrelated source N

Consider the i'th and j'th microphones, a single point acoustic source A and a noise source N.
As shown in Appendix A, the auto spectra are

$$G_{p_{a_i} p_{a_i}} = \frac{1}{2} \frac{A^2}{R_{a_i}^2} \delta(f - f_0) + \frac{1}{2} \frac{B^2}{R_{b_i}^2} \delta(f - f_0) + \frac{1}{2} \frac{N^2}{R_{n_i}^2} \delta(f - f_0) \tag{31}$$

$$G_{p_{a_j} p_{a_j}} = \frac{1}{2} \frac{A^2}{R_{a_j}^2} \delta(f - f_0) + \frac{1}{2} \frac{B^2}{R_{b_j}^2} \delta(f - f_0) + \frac{1}{2} \frac{N^2}{R_{n_j}^2} \delta(f - f_0) \tag{32}$$

and the cross spectrum is

$$G_{p_i p_j} = \frac{1}{2} \frac{A^2}{R_{a_i} R_{a_j}} e^{-jk(R_{a_i} - R_{a_j})} \delta(f - f_0) + \frac{1}{2} \frac{B^2}{R_{b_i} R_{b_j}} e^{-jk(R_{b_i} - R_{b_j})} \delta(f - f_0) \tag{33}$$
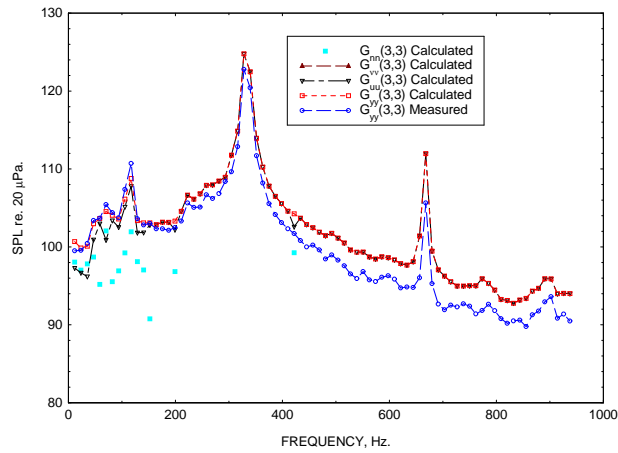
(a) Auto-spectrum 100 Degree microphone at 150 feet using three parameter model.
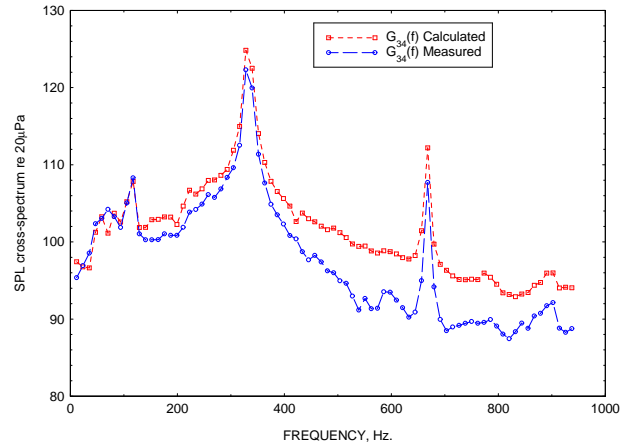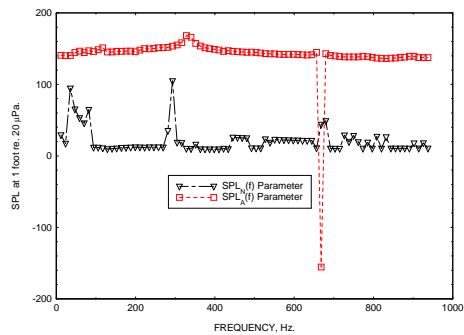

(b) Cross-spectrum magnitude between 100 and 110 Degree microphones at 150 feet using three parameter model.
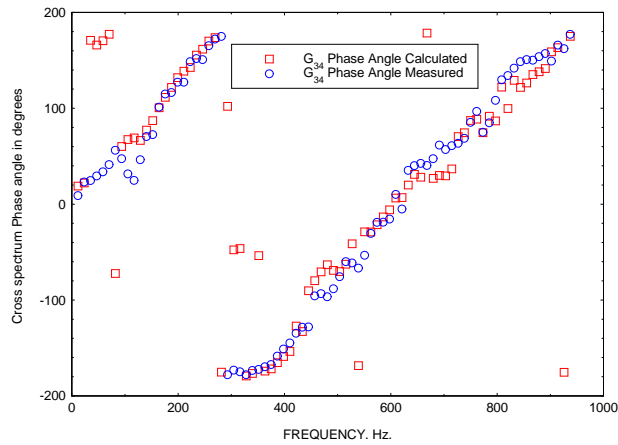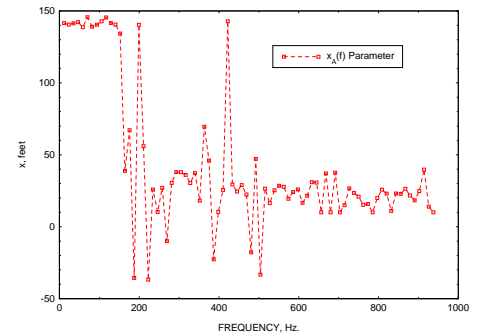

(c) Cross-spectrum phase angle between 100 and 110 Degree microphones at 150 feet using three parameter model
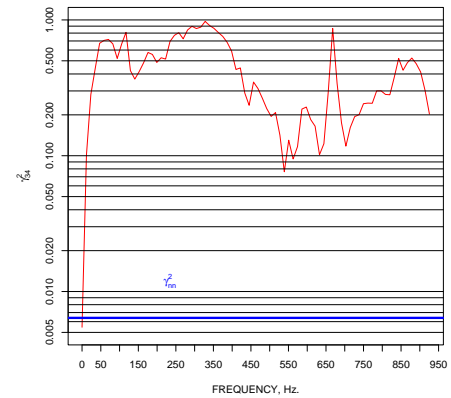
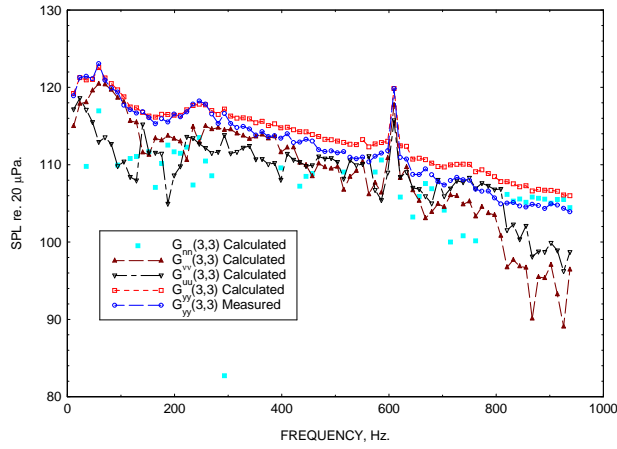(d) Coherence between 100 and 110 Degree microphones at 150 feet

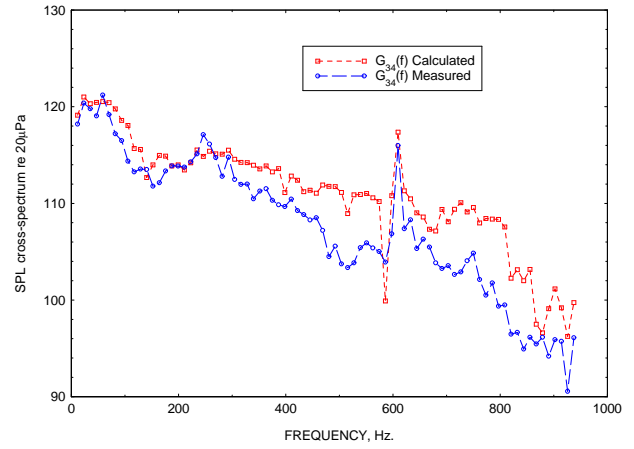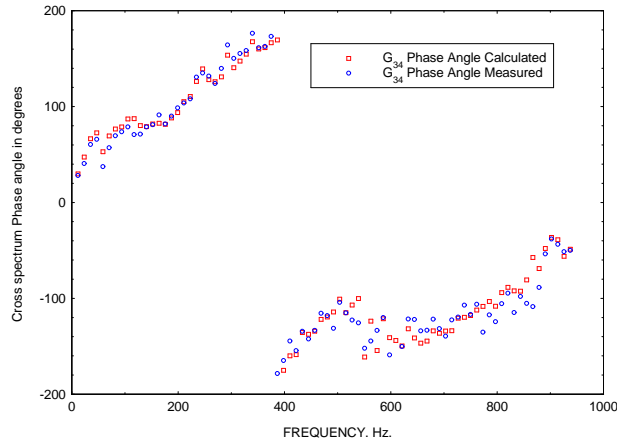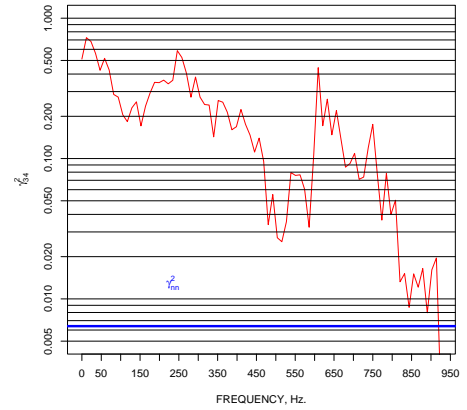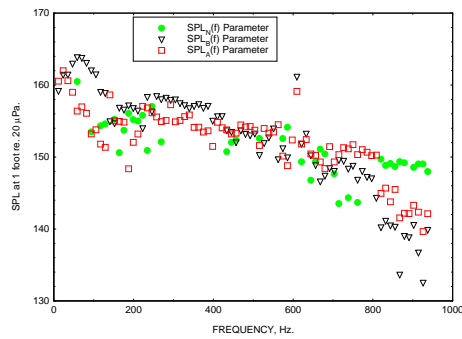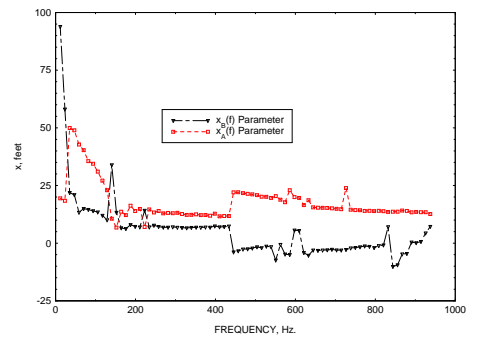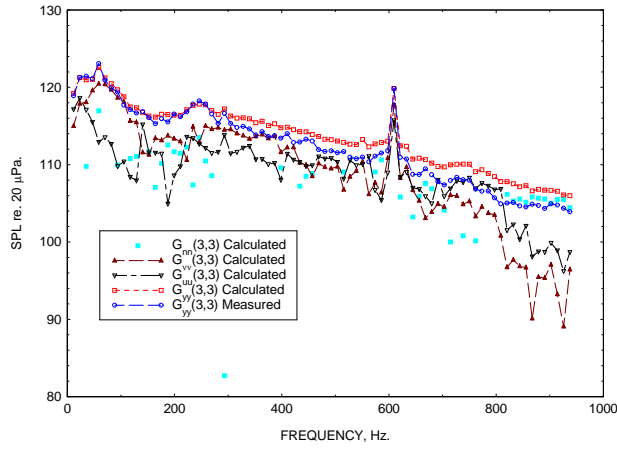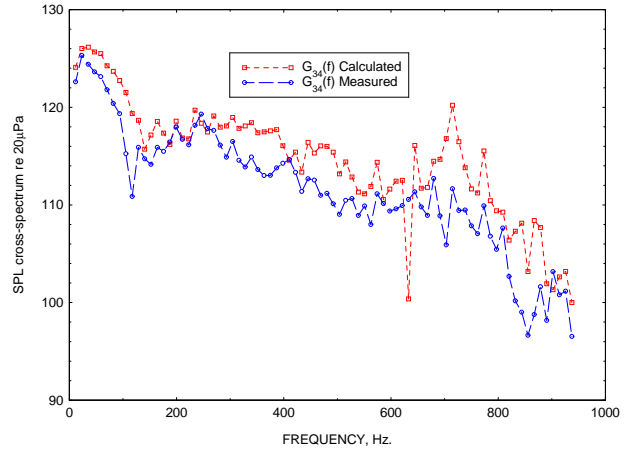(e) SPL_A and SPL_N parameters for three parameter model.

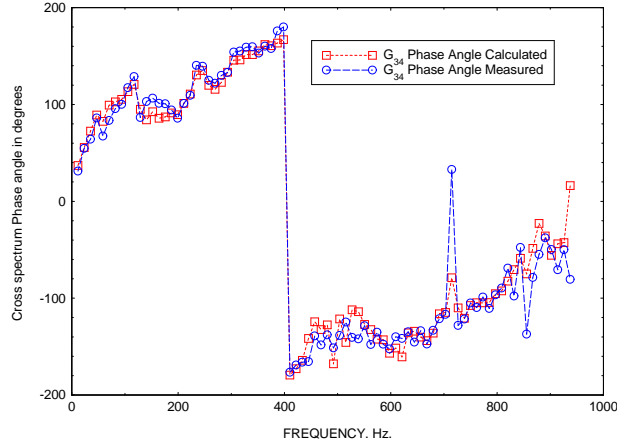(f) x_A location parameter for three parameter model
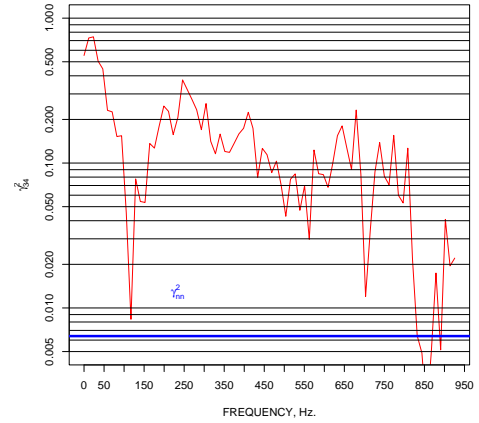
Figure 4.   582 rpm (N1 Corr.).

(a) Auto-spectrum 100 Degree microphone at 150 feet using five parameter model.
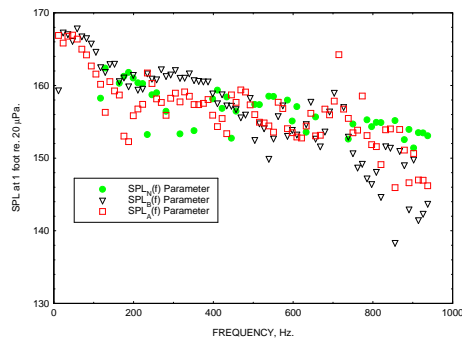

(b) Cross-spectrum magnitude between 100 and 110 Degree microphones at 150 feet using five parameter model.

(c) Cross-spectrum phase angle between 100 and 110 Degree microphones at 150 feet using five parameter model.

(d) Coherence between 100 and 110 Degree microphones at 150 feet

(e) SPL_A, SPL_B and SPL_N parameters for five parameter model.

(f) x_A location parameter and x_B location parameters for five parameter model.

Figure 5. 1622 rpm (N1 Corr.).

(a) Auto-spectrum 100 Degree microphone at 150 feet using five parameter model.

(b) Cross-spectrum magnitude between 100 and 110 Degree microphones at 150 feet using five parameter model.
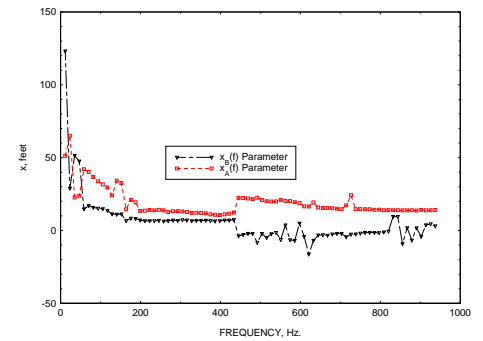
(c) Cross-spectrum phase angle between 100 and 110 Degree microphones at 150 feet using five parameter model.

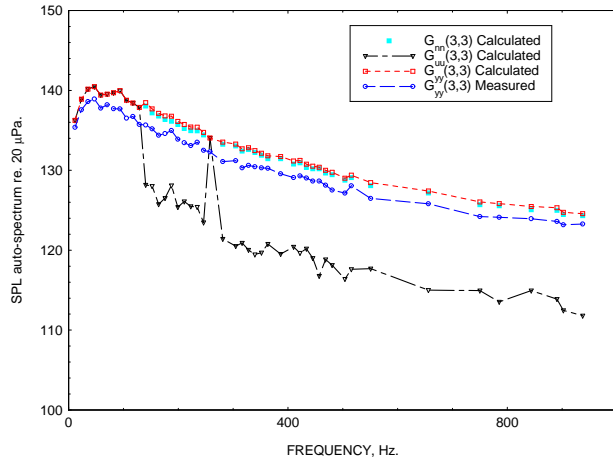(d) Coherence between 100 and 110 Degree microphones at 150 feet

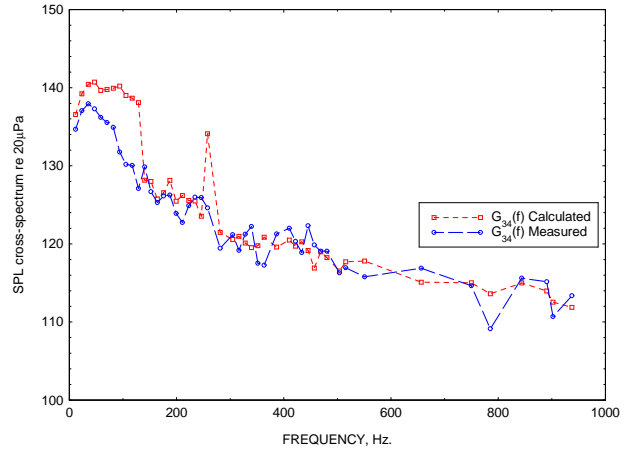(e) SPL_A, SPL_B and SPL_N parameters for five parameter model.

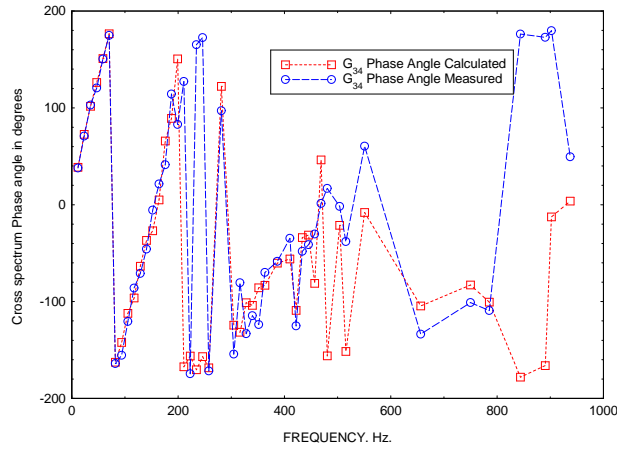(f) x_A location parameter and x_B location parameters for five parameter model.
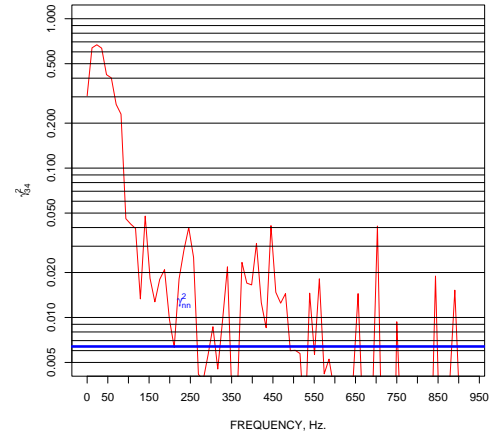
Figure 6. 1900 rpm.(N1 Corr.)

(a) Auto-spectrum 100 Degree microphone at 150 feet using three parameter model.

(b) Cross-spectrum magnitude beteen 100 and 110 Degree microphones at 150 feet using three parameter model.

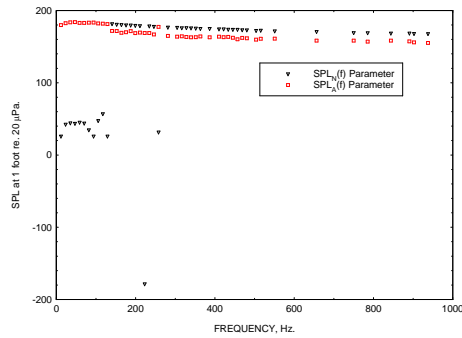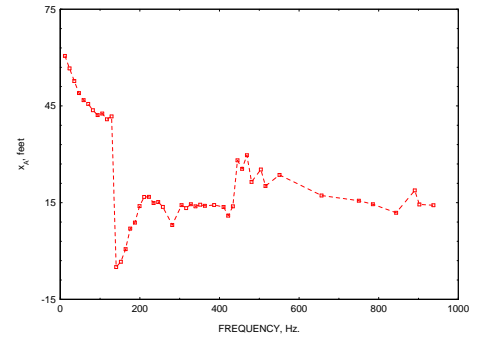(c) Cross-spectrum phase angle between 100 and 110 Degree microphones at 150 feet using three parameter model.

(d) Coherence between 100 and 110 Degree microphones at 150 feet

(e) SPL_A and SPL_N parameters for three parameter model.

(f) x_A location parameter for three parameter model.

Figure 7.   2743 rpm. (N1 Corr.)

References

[1] Jeffrey Hilton Miles. Aligned and unaligned coherence: A new diagnostic tool. AIAA-2006-0010, NASA/TM–2006-214112, January 2006.

[2] Jeffrey Hilton Miles. Validating coherence measurements using aligned and unaligned coherence functions. AIAA-2006-1389, NASA/TM–2006-214113, January 2006.

[3] Jeffrey Hilton Miles. Restricted acoustic modal analysis applied to internal combustor spectra and cross-spectra measurements. AIAA-2006-2581, May 2006.

[4] Julius S. Bendat and Allan G. Piersol. *Measurement and Analysis of Random Data*. John Wiley &Sons, 1966.

[5] Julius S. Bendat and Allan G. Piersol. *Random Data: Analysis and Measurement Procedures*. John Wiley &Sons, 1971.

[6] Julius S. Bendat and Allan G. Piersol. *Engineering Applications of Correlation and Spectral Analysis*. John Wiley &Sons, 1980.

[7] Allen M. Karchmer. Identification and measurement of combustion noise from a turbofan engine using correlation and coherence techniques. NASA TM-73747, 1977.

[8] A.M. Karchmer, M. Reshotko, and F.J. Montegani. Measurement of far field combustion noise from a turbofan engine using coherence functions. AIAA Paper 77-1277,NASA TM-73748, Oct. 1977.

[9] J. Y. Chung, Malcolm J. Crocker, and James F. Hamiton. Measurement of frequency response and the multiple coherence function of the noise-generation system of a diesel engine. *J. Acoust. Soc. Am.*, **58** No. 3:636–642, September 1975.

[10] J. Y. Chung. Rejection of flow noise using a coherence function method. *J. Acoust. Soc. Am.*, **62** No. 2:388–395, August 1977.

[11] Eugene A. Krejsa. New technique for the direct measurement of core noise from aircraft engines. Technical Report TM-82634, NASA, 1981.

[12] Belur N. Shivashankara. High bypass ratio engine noise component separation by coherence technique. *J. Aircraft*, **20** No. 3:236–242, March 1983. AIAA 81-2054, Aeroacoustics Conference, 7th, Palo Alto, CA Oct. 5-7, 1981.

[13] J.S. Hsu and K. K. Ahuja. A coherence-based technique to separate ejector internal mixing noise from farfield measurements. AIAA-98-2296, June 1998.

[14] R. W. Stoker, K. K. Ahuja, and J. HJsu. Separation of wind-tunnel background noise and wind noise from automobile interior measurements. AIAA-96-1763, May 1996.

[15] A. Michalke, F. Arnold, and F. Holste. On the coherence of the sound field in a circular duct with uniform mean flow. *Journal of Sound and Vibration*, **190** No. 2:261–271, 1996.

[16] Tomoyuki Minami and K. K. Ahuja. Five-microphone method for separating two different correlated noise sources from far field measurements contaminated by extraneous noise. AIAA 2003-3261, May 2003.

[17] S.P.Parthasarathy, R.F.Cuffel, and P.F.Massier. Separation of core noise and jet noise. *AIAA Journal*, **18** No. 3:256–261, 1980. AIAA-79-0589.

[18] Vincent Tesson. *Experimental Investigation of Jet Noise and Core Noise Using a Small Gas Turbine Engine*. A master of science thesis in aerospace engineering, The Pennsylvania State University, Department of Aerospace Engineering, August 2002.

[19] Vincent Tesson. Experimental investigation of jet noise and core noise using a small gas turbine engine. AIAA-2002-2558, June 2002.

[20] Richard P. Brent. *Algorithms for Minimization Without Derivatives*. Prentice-Hall,1973;Dover Pulications, 2002, 1973, 2002.

[21] M. J. D. Powell. An efficient method of finding the mibnimum of a function of several variables without calculating derivatives. *Computer Journal*, **7** No. 2:155–162, July 1964.

[22] M. S. Shapiro and M. Goldstein. A collection of mathematical computer routines. Technical Report NYU-1480-14, New York University, February 1965.

[23] James L. Kuester and Joe H. Mize. *Optimization Techniques with Fortran*. McGraw-Hill, 1973.

[24] Samuel D. Stearns and Ruth A. David. *Signal Processing Algorithms Using Fortran and C*. PTR Prentice-Hall, Inc., 1993.

[25] G. Clifford Carter. Receiver operating characteristics for a linearly thresholded coherence estimation detector. *IEEE Transactions on Acoustics, Speech, and Signal Processing*, **ASSP-25** :90–92, February 1977.

[26] G. Clifford Carter. Coherence and time dealy estimation. *Proceedings of the IEEE*, **75** No. 2:236–255, February 1987.

[27] DM Halliday, JR Rosenberg, AM Amjad, P Breeze, BA Conway, and SF Farmer. A framework for the analysis of mixed time series/point process data-theory and application to the study of physiological tremor. *Prog. Biophys Mol Biol*, **64** No.:237–278, 1995.

[28] David R. Brillinger. *Time Series Data Analysis and Theory -Expanded Edition*. Holden-Day, 1981. ISBN:0-8162-1150-7.

[29] Allan Piersol. Time delay estimation using phase data. *IEEE Transactions on Acoustics, Speech, and Signal Processing*, **ASSP-29** No. 3:471–477, June 1981.

[30] Philip M. Morse and K. Uno Ingard. *Theoretical Acoustics*. McGraw-Hill Book Company, 1968.

REPORT DOCUMENTATION PAGE

Public reporting burden for this collection of information is estimated to average 1 hour per response, including the time for reviewing instructions, searching existing data sources, gathering and maintaining the data needed, and completing and reviewing the collection of information. Send comments regarding this burden estimate or any other aspect of this collection of information, including suggestions for reducing this burden, to Washington Headquarters Services, Directorate for Information Operations and Reports, 1215 Jefferson Davis Highway, Suite 1204, Arlington, VA 22202-4302, and to the Office of Management and Budget, Paperwork Reduction Project (0704-0188), Washington, DC 20503.

1. AGENCY USE ONLY (Leave blank)	2. REPORT DATE	3. REPORT TYPE AND DATES COVERED
	May 2006	Technical Memorandum

4. TITLE AND SUBTITLE

Procedure for Separating Noise Sources in Measurements of Turbofan Engine Core Noise

5. FUNDING NUMBERS

WBS 561581.02.08.03

6. AUTHOR(S)

Jeffrey Hilton Miles

7. PERFORMING ORGANIZATION NAME(S) AND ADDRESS(ES)

National Aeronautics and Space Administration
John H. Glenn Research Center at Lewis Field
Cleveland, Ohio 44135–3191

8. PERFORMING ORGANIZATION REPORT NUMBER

E–15627

9. SPONSORING/MONITORING AGENCY NAME(S) AND ADDRESS(ES)

National Aeronautics and Space Administration
Washington, DC 20546–0001

10. SPONSORING/MONITORING AGENCY REPORT NUMBER

NASA TM—2006-214352
AIAA–2006–2580

11. SUPPLEMENTARY NOTES

Prepared for the 12th Aeroacoustics Conference cosponsored by the American Institute of Aeronautics and Astronautics and Confederation of European Aerospace Societies, Cambridge, Massachusetts, May 8–10, 2006. Responsible person Jeffrey Hilton Miles, organization code RTA, 216–433–5909.

12a. DISTRIBUTION/AVAILABILITY STATEMENT

Unclassified - Unlimited
Subject Category: 35

Available electronically at http://gltrs.grc.nasa.gov

This publication is available from the NASA Center for AeroSpace Information, 301–621–0390.

12b. DISTRIBUTION CODE

13. ABSTRACT (Maximum 200 words)

The study of core noise from turbofan engines has become more important as noise from other sources like the fan and jet have been reduced. A multiple microphone and acoustic source modeling method to separate correlated and uncorrelated sources has been developed. The auto and cross spectrum in the frequency range below 1000 Hz is fitted with a noise propagation model based on a source couplet consisting of a single incoherent source with a single coherent source or a source triplet consisting of a single incoherent source with two coherent point sources. Examples are presented using data from a Pratt & Whitney PW4098 turbofan engine. The method works well.

14. SUBJECT TERMS

Combustion noise; Core noise; Noise source separation

15. NUMBER OF PAGES

24

16. PRICE CODE

17. SECURITY CLASSIFICATION OF REPORT	18. SECURITY CLASSIFICATION OF THIS PAGE	19. SECURITY CLASSIFICATION OF ABSTRACT	20. LIMITATION OF ABSTRACT
Unclassified	Unclassified	Unclassified	

NSN 7540-01-280-5500

Standard Form 298 (Rev. 2-89)
Prescribed by ANSI Std. Z39-18
298-102